

PDF hosted at the Radboud Repository of the Radboud University Nijmegen

The following full text is a publisher's version.

For additional information about this publication click this link.

<http://hdl.handle.net/2066/75795>

Please be advised that this information was generated on 2017-12-06 and may be subject to change.

Ellipsoidal InAs quantum dots observed by cross-sectional scanning tunneling microscopy

J. H. Blokland,¹ M. Bozkurt,² J. M. Ulloa,² D. Reuter,³ A. D. Wieck,³ P. M. Koenraad,² P. C. M. Christianen,^{1,a)} and J. C. Maan¹

¹High Field Magnet Laboratory, Institute for Molecules and Materials, Radboud University Nijmegen, Toernooiveld 7, 6525 ED Nijmegen, The Netherlands

²Department of Applied Physics, COBRA Inter-University Research Institute, Eindhoven University of Technology, P.O. Box 513, 5600 MB Eindhoven, The Netherlands

³Lehrstuhl für Angewandte Festkörperphysik, Ruhr-Universität Bochum, D-44799 Bochum, Germany

(Received 11 November 2008; accepted 23 December 2008; published online 15 January 2009)

We report a detailed analysis of the shape, size, and composition of self-assembled InAs quantum dots based on cross-sectional scanning tunneling microscopy (X-STM) experiments. X-STM measurements on 13 individual quantum dots reveal an ellipsoidal dot shape with an average height of 8 nm and a diameter of 26 nm. Analysis of the outward relaxation and lattice constant profiles shows that the dots consist of an InGaAs alloy with a profound gradient in the indium concentration in both horizontal and vertical directions. These results are important to obtain a deeper understanding of the relationship between the structural and electronic properties of semiconductor quantum dots. © 2009 American Institute of Physics. [DOI: 10.1063/1.3072366]

The physical properties of nanosized objects such as semiconductor quantum dots (QDs) strongly depend on their actual dimensions and composition. To fully exploit QDs for advanced applications^{1,2} and to better understand the underlying physics, it is therefore important to investigate this structure-property relationship. In many studies on epitaxial QDs, however, there is only limited information on their structure,^{3–6} and in order to describe those experiments an idealized QD shape and composition had to be assumed. This lack of information hinders a thorough interpretation of experimental results and limits the applicability of theoretical calculations.^{7–9} Recent progress in advanced structural characterization techniques made it possible to determine the shape and composition of In(Ga)As QDs, demonstrating a large variety in shape: lens-shaped dots found by tunneling electron microscopy,^{10,11} pyramid-shaped dots by cross-sectional scanning tunneling microscopy (X-STM) (Ref. 12) and more complicated faceted shapes by STM.¹³ A major advantage of X-STM is that it is able to characterize QDs embedded in a matrix, which can be substantially different from those at the sample surface, as measured by atomic force microscopy and STM.¹⁴ Indeed, X-STM experiments on embedded InAs QDs (Ref. 15) and quantum rings¹⁶ have shown that their actual electronic properties could only be explained by the unexpected geometry and composition of nano-objects.

Here we present X-STM measurements on *p*-type InAs QDs, which are physically very relevant to understand few-particle effects in quantum confined systems.^{17–19} We find an unprecedented ellipsoidal shape with a large indium gradient in both vertical and horizontal directions. This result can be used as input for realistic models to better understand the charging characteristics and optical properties of semiconductor QDs.

The sample used consists of a *p*-doped GaAs back contact, followed by a 19 nm undoped GaAs tunneling barrier, a

single InAs QD layer, a 19 nm thick GaAs tunneling barrier, an AlAs/GaAs superlattice, and a GaAs cap layer. The QD layer was grown by 15 repetitions of 0.2 nm InAs at a temperature of 525 °C. The wafer was rotated during the growth procedure. This sample is identical¹⁹ or similar^{17,20,21} to those previously studied using photoluminescence (PL) and capacitance-voltage (*CV*) spectroscopy. The 4.2 K PL spectrum is centered around an energy of 1.07 eV with a full width at half maximum of 26 meV. *CV* spectroscopy reveals up to six clear charging peaks that correspond to the sequential filling of the QDs by single holes.^{17,19} The relatively narrow PL lines and the observation of individual charging peaks evidence the large uniformity of the QDs. We estimate an inhomogeneous size distribution of only 5%. X-STM measurements have been conducted at room temperature in an ultra high vacuum chamber ($p < 4 \times 10^{-11}$ Torr) on the (*in situ* cleaved) [011] cross-sectional surface. Polycrystalline tungsten tips prepared by electrochemical etching have been used. The images have been taken at high voltage (~ 3.0 V) to suppress the electronic contrast and to enhance the topographic contrast due to the outward relaxation.²² After cleavage of the sample, the indium-rich regions relax out of the GaAs matrix due to the strain caused by the 7% lattice constant mismatch between GaAs and InAs. Determining the outward relaxation thus provides a measure for the local indium content inside the dot.

We investigated 13 individual QDs originating from a piece of the wafer next to the part that has been used for PL and *CV* measurements.¹⁹ Representative topography images are shown in Fig. 1(c) (after Fourier filtering to highlight the atomic layers) and Fig. 2(b) (as measured). These images represent the QD with the largest measured height of 8.1 ± 0.4 nm with a diameter of 27.5 ± 4 nm. Figure 1(b) shows the height-base diameter distribution for all 13 dots, where the tallest dot [Fig. 1(c)] corresponds to the encircled data point. The height-base diameter statistics contains important information on the average shape of the QDs. Considering their high uniformity we assume that all dots are

^{a)}Electronic mail: p.christianen@science.ru.nl.

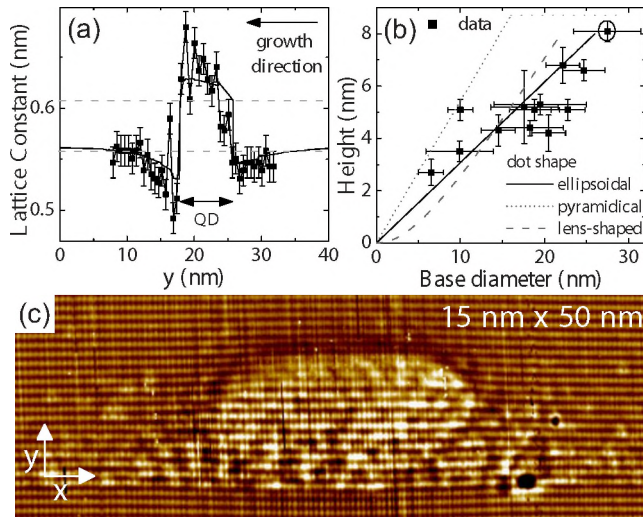


FIG. 1. (Color online) (a) Measured (symbols) and calculated (line) lattice constant profiles through the middle plane in the growth direction of an InAs QD. The dashed lines indicate the lattice constant of bulk InAs (0.61 nm) and GaAs (0.56 nm). (b) Height vs base diameter for the 13 measured QDs (symbols). Theoretical curves for ellipsoidal (solid line, height $h=8$ nm, diameter $d=26$ nm), pyramidal (dotted line, $h=8.7$ nm, base $b=29$ nm) and lens-shaped QDs (dashed line, $h=8$ nm, $d=22$ nm). (c) Fourier filtered topography image of a representative QD assumed to be cleaved through its middle plane. This dot corresponds to the encircled data point in (b).

identical. The measured height and base diameter then merely depend on the cleavage plane through the dot, occurring at random positions. For instance, the dot with the largest measured height is thought to be cleaved through its middle plane, whereas the others are cleaved closer to the edge. Each dot shape has therefore a specific height-base

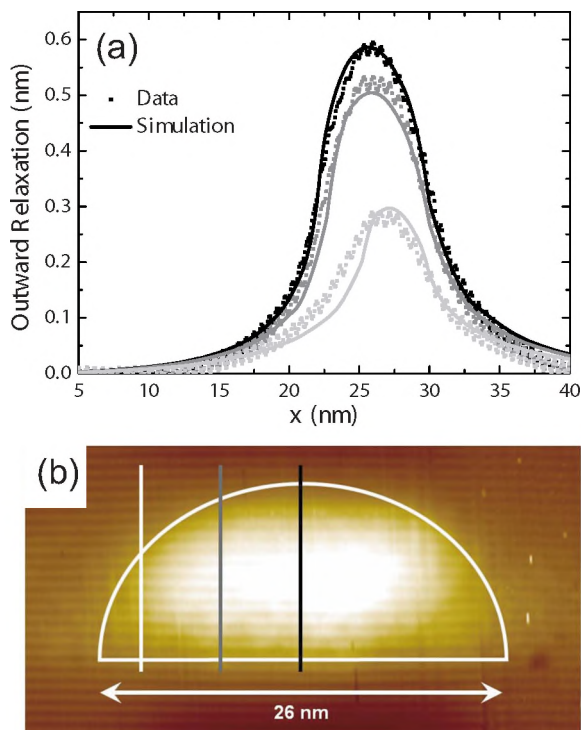


FIG. 2. (Color online) (a) Measured (symbols) and simulated (solid lines) outward relaxation at three different positions with respect to the middle of an InAs QD. (b) Topography image of the tallest QD measured. The z -range of this image is 0.7 nm. The solid lines indicate the positions at which the outward relaxation is plotted in (a).

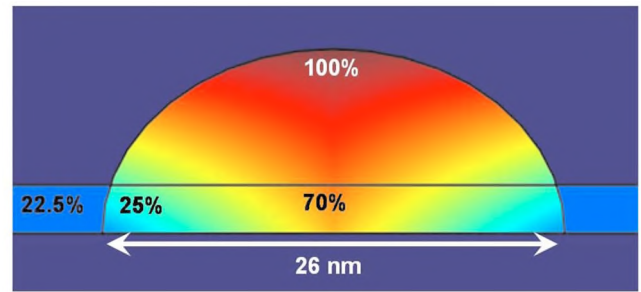


FIG. 3. (Color online) Simulated indium content of a InAs QD. The color scale indicates the percentage of indium arsenide composition and the given numbers correspond to the end values at the top center, base center, base edge, and WL.

diameter relationship. Remarkably, the statistics of the 13 dots strongly deviates from a pyramidal shape (dotted line), previously found by X-STM.^{12,22} Better agreement is found using a lens-shape (dashed line) or ellipsoidal (solid line) QD, which agrees well with the topography of the dot [outlined in Fig. 2(b)].

To obtain a full characterization of the QD shape and composition we performed a detailed analysis of the representative dot in Figs. 1(c) and 2(b). In particular, the indium concentration profile follows from analysis of the lattice constant [Fig. 1(a)] and the outward relaxation [Fig. 2(a)]. The lattice constant is determined in the middle of the dot by taking line profiles across the cleaved surface and measuring the distances between the atom rows, using the Fourier filtered topography image [Fig. 1(c)]. The lattice constant increases from the GaAs value at the bottom of the dot to the InAs value at the top.

The measured outward relaxation at different lateral positions in the cleavage plane [cf. Fig. 2(b)] is compared with simulations [Fig. 2(a)]. The simulation is performed with finite element calculations based on continuum elasticity theory. In these calculations the QD consist of an InGaAs alloy, in which the internal indium concentration profile is described by an expression that uses the indium end concentrations at different points inside the dot and using linear interpolation in between. The dot is assumed to be surrounded by a pure GaAs matrix and is on top of a seven monolayer thick $\text{In}_{0.225}\text{Ga}_{0.775}\text{As}$ wetting layer (WL). The thickness of the WL has been determined experimentally by X-STM at a position far from a QD (not shown) and agrees well with a total indium content of 1.7 ML.

Comparing the measured and modeled outward relaxation, we obtain excellent agreement with an ellipsoidal dot, whose shape is described by the equation $(x/13)^2 + (y/8)^2 = 1$ (dimensions in nm) and with the indium profile depicted in Fig. 3. The indium concentration varies significantly over the dot. The fraction InAs increases vertically from 70% at the base center to 100% at the top center. In addition, horizontally the fraction InAs decreases to 25% at the base edge, evolving in a 22.5% 7 ML thick WL. These dot parameters nicely reproduce the variation in the lattice constant in going from bottom center to top center as shown by the solid line in Fig. 1(a), which is further evidence of the large gradients in indium content.

It is important to note that this level of agreement between simulation and data could not be obtained with a lens-shaped dot or using an ellipsoidal dot without WL. The

present simulations thus represent the simplest dot shape and composition that matches the data. More complicated faceted dots¹³ cannot be disregarded but additional minor changes in the dot shape would not greatly influence the results we have found. Our relatively tall dots with large indium gradients differ significantly from some of the dots previously used in calculations, where usually a fixed InAs fraction is assumed.

Linking this geometry and composition to the previously performed PL and hole charging experiments in high magnetic fields on the *same* sample¹⁹ requires a sophisticated model, which is beyond the scope of this paper. However, by qualitative arguments we are able to explain the PL emission energy of these dots. In view of the strong indium gradient found in these dots and the fact that the energy gap of InAs is lower than that of GaAs, the wave function is expected to be localized primarily in the top (indium rich) region of the QDs. This would reduce both the effective height and the effective diameter that have to be used as input parameters in a simplified model to calculate the emission energy. Furthermore, our measured geometry can be used as input for calculations to determine the hole charging sequence and the character of the hole wave functions, which are still under debate.

In conclusion, we measured the shape, size, and composition of self-assembled InAs QDs in a GaAs matrix. We found that the dot shape is best described by an ellipsoid with a strong indium gradient in both horizontal and vertical directions. This conclusion is supported by the outward relaxation and lattice constant profiles across the dot, and by the height-base diameter statistics on 13 individual QDs. These results are crucial for a more thorough understanding of the influence of the dot's geometry on its spectroscopic properties.

This work is partly sponsored by DeNUF, EU FP6 Contract No. 011760.

¹Y. Arakawa and H. Sakaki, *Appl. Phys. Lett.* **40**, 939 (1982).

²Z. Yuan, B. E. Kardynal, R. M. Stevenson, A. J. Shields, C. J. Lobo, K. Cooper, N. S. Beattie, D. A. Ritchie, and M. Pepper, *Science* **295**, 102 (2002).

³R. J. Warburton, B. T. Miller, C. S. Durr, C. Bodefeld, K. Karrai, J. P. Kotthaus, G. Medeiros-Ribeiro, P. M. Petroff, and S. Huan, *Phys. Rev. B*

58, 16221 (1998).

⁴S. Raymond, S. Studenikin, A. Sachrajda, Z. Wasilewski, S. J. Cheng, W. Sheng, P. Hawrylak, A. Babinski, M. Potemski, G. Ortner, and M. Bayer, *Phys. Rev. Lett.* **92**, 187402 (2004).

⁵A. Babinski, M. Potemski, S. Raymond, J. Lapointe, and Z. R. Wasilewski, *Phys. Rev. B* **74**, 155301 (2006).

⁶U. Banin, Y. Cao, D. Katz, and O. Millo, *Nature (London)* **400**, 542 (1999).

⁷G. A. Narvaez, G. Bester, and A. Zunger, *J. Appl. Phys.* **98**, 043708 (2005).

⁸Z. R. Wasilewski, S. Fafard, and J. P. McCaffrey, *J. Cryst. Growth* **201**, 1131 (1999).

⁹A. Schliwa, M. Winkelkemper, and D. Bimberg, *Phys. Rev. B* **76**, 205324 (2007).

¹⁰T. Walther, A. G. Cullis, D. J. Norris, and M. Hopkinson, *Phys. Rev. Lett.* **86**, 2381 (2001).

¹¹D. Leonard, M. Krishnamurthy, C. M. Reaves, S. P. Denbaars, and P. M. Petroff, *Appl. Phys. Lett.* **63**, 3203 (1993).

¹²D. M. Bruls, J. W. A. M. Vugs, P. M. Koenraad, H. W. M. Salemink, J. H. Wolter, M. Hopkinson, M. S. Skolnick, F. Long, and S. P. A. Gill, *Appl. Phys. Lett.* **81**, 1708 (2002).

¹³G. Costantini, A. Rastelli, C. Manzano, P. Acosta-Diaz, G. Katsaros, R. Songmuang, O. Schmidt, H. v. Kanel, and K. Kern, *J. Cryst. Growth* **278**, 38 (2005).

¹⁴P. Offermans, P. M. Koenraad, J. H. Wolter, D. Granados, J. M. Garcia, V. M. Fomin, V. N. Gladilin, and J. T. Devreese, *Appl. Phys. Lett.* **87**, 131902 (2005).

¹⁵P. W. Fry, I. E. Itskevich, D. J. Mowbray, M. S. Skolnick, J. J. Finley, J. A. Barker, E. P. O'Reilly, L. R. Wilson, I. A. Larkin, P. A. Maksym, M. Hopkinson, M. Al-Khafaji, J. P. R. David, A. G. Cullis, G. Hill, and J. C. Clark, *Phys. Rev. Lett.* **84**, 733 (2000).

¹⁶N. A. J. M. Kleemans, I. M. A. Bomiñaar-Silkens, V. M. Fomin, V. N. Gladilin, D. Granados, A. G. Taboada, J. M. Garcia, P. Offermans, U. Zeitler, P. C. M. Christianen, J. C. Maan, J. T. Devreese, and P. M. Koenraad, *Phys. Rev. Lett.* **99**, 146808 (2007).

¹⁷D. Reuter, P. Kailuweit, A. D. Wieck, U. Zeitler, O. Wibbelhoff, C. Meier, A. Lorke, and J. C. Maan, *Phys. Rev. Lett.* **94**, 026808 (2005).

¹⁸G. Bester, D. Reuter, L. He, A. Zunger, P. Kailuweit, A. D. Wieck, U. Zeitler, J. C. Maan, O. Wibbelhoff, and A. Lorke, *Phys. Rev. B* **76**, 075338 (2007).

¹⁹J. H. Blokland, F. J. P. Wijnen, P. C. M. Christianen, U. Zeitler, J. C. Maan, P. Kailuweit, D. Reuter, and A. D. Wieck, *Phys. Rev. B* **75**, 233305 (2007).

²⁰D. Reuter, P. Schafmeister, P. Kailuweit, and A. D. Wieck, *Physica E* **21**, 445 (2004).

²¹D. Reuter, P. Kailuweit, A. D. Wieck, U. Zeitler, and J. C. Maan, *Physica E* **26**, 446 (2005).

²²J. M. Ulloa, C. Celebi, P. M. Koenraad, A. Simon, E. Gapihan, A. Letoublon, N. Bertru, I. Drouzas, D. J. Mowbray, M. J. Steer, and M. Hopkinson, *J. Appl. Phys.* **101**, 081707 (2007).